Electronic supplementary information

for

Distinct mechanisms for the pro-apoptotic conformational transition and alkaline transition in cytochrome *c*

Tianlei Ying[#], Zhong-Hua Wang[#], Fangfang Zhong, Xiangshi Tan* and Zhong-Xian Huang*

Materials

The plasmid pBTR1 was a gift from Professor A.G. Mauk. Pfu DNA polymerase was purchased from New England Biolabs. The plasmid preparation kit was purchased from Qiagen. QuikChange Site-Directed Mutagenesis Kit was the product of Stratagene. The *E. coli* strain BL21(DE3)pLysS was obtained from Novagen. CM-52 and CM Sepharose Fast Flow resin were purchased from Whatman and Pharmacia, respectively. All other reagents were of analytic grade.

Protein Preparation

The original pBTR1 plasmid, which encodes genes of the yeast iso-1-cytochrome *c* (*CYC*1) and yeast cytochrome *c* heme lyase (*CYC*3), has the native Cys102 residue substituted by a threonine residue to prevent formation of disulphide bonds between cyt *c* molecules, and also contains a mutation of K72A to prevent this residue to serve as a ligand in the alkaline form of the protein.[S1, S2] For the purpose of this work, this variant is used as the reference cytochrome and is referred to as wild-type protein (cytochrome *c*, cyt *c*). The construction of Y67H variant was described previously.[11] The Y67H/M80V and Y67H/M80D mutants were constructed based on the Y67H plasmid with the QuickChange Site-Directed Mutagenesis Kit (Stratagene), according to the manufacturer's protocol. The oligonucleotides used were as follows with mutant codon(s) underlined:

FM-primer for Y67H/M80V:

5'- TCCTGGTACCAAG<u>GT</u>GGCCTTTGGTGGG -3',

RM-primer for Y67H/M80V:

5'- CCCACCAAAGGCCA<u>C</u>CTTGGTACCAGGA -3';

FM-primer for Y67H/M80D:

5'- GCGAAATATATTCCTGGTACCAAGG<u>AT</u>GCCTTTGGTGGGTTGAAGAAGG -3'

RM-primer for Y67H/M80D:

5'- CCTTCTTCAACCCACCAAAGGC<u>AT</u>CCTTGGTACCAGGAATATATTTCGC -3'

The plasmid was PCR amplified in the elongation process using *PfuTurbo* DNA polymerase according to the manufacture's protocol. The incorporation of the two oligonucleotides primers generates the mutated plasmid containing stagger nicks. The product was then treated with *Dpn* I restriction enzyme, specific for methylated and hemimethylated DNA, then the parental DNA template was digested (almost all DNA isolated from commonly *E. coli* strains is usually dam methylated). The nicked vector DNA containing the desired mutations was then transformed into XL1–Blue super-competent cells. The plasmid DNA was isolated using a QIAprep Spin Miniprep Kit (Qiagen) and the identity of the mutants were confirmed by DNA sequencing.

Expression and purification of the variants were performed according to the methods described previously[S1-S2] with modifications.

Cultures were initiated with a single, freshly transformed *E. coli* BL21(DE3)pLysS that served as the inoculum for 50 mL SB media supplemented with 100 mg/mL ampicillin to 0.1% (V/V). After overnight incubation at 37 °C with vigorous shaking (300 rpm), 5 mL was used to inoculate 800 mL modified SB (tryptone: 10 g/L, yeast extract: 8 g/ L, sodium chloride: 5 g/L, glycerin: 1.5 mL/L, sodium nitrate: 4 g/ L) with 100 mg/L ampicillin in a 1 liter flask and were incubated for 24-32 hrs. The cells were harvested by centrifugation (Sorvall SLA-3000 rotor, 4 °C, 5000 rpm, 15 min) and resuspended in lysis buffer (50 mM Tris-HCl, 1 mM EDTA, pH 8.0) with 3 g/L lysozyme and a few crystals of DNase I and RNase A. The mixture was stirred continuously for 1 hour at 4 °C, and then lysed by sonication on ice. This lysate was cleared by centrifugation (Sorvall SS-34 rotor, 4 °C, 15000 rpm, 20 min), and the resulting solution was collected. The pellet was resuspended in lysis buffer and centrifugated repeatedly until the pellet and the supernatant were no longer pink. The colored fractions were pooled, and $(NH_4)_2SO_4$ (15% w/v) was added over a period of 30 min while stirring gently at 4 °C. The resulting suspension was centrifuged before dialyzing the supernatant fluid overnight in distilled water (4 °C). The dialysate was centrifuged again, and the protein in the cleared solution was loaded on a column of CM-52 cation exchange resin equilibrated with Buffer A (50 mM sodium phosphate, pH 6.8). After loading, the column was washed with two volumes of Buffer A followed by two volumes of Buffer B (Buffer A plus 75 mM NaCl). Then the protein was eluted with Buffer C (Buffer A plus 250 mM NaCl) and exchanged into Buffer A by repeated

ultrafiltration with YM-10 membrane (Amicon). Samples were oxidized with $K_3[Fe(CN)_6]$ immediately prior to the final purification by cation exchange chromatography with a CM Sepharose Fast Flow column equilibrated with sodium phosphate buffer (20 mM, pH 7.0). The protein was eluted with a linear NaCl gradient of 1-300 mM/mL, Fractions with the R-value (A_{408}/A_{280}) > 5 were pooled, concentrated, and exchanged into Buffer A prior to flash-freezing in liquid nitrogen, lyophilized and storage at −80 °C until needed.

Mass spectroscopy

Molecular weight of the proteins were measured by electrospray ionization mass spectrometry (ESI-MS) using a Bruker Esquire 3000 Electrospray Mass Spectrometer (Bruker Daltonicsk Germany). The protein solutions were first desalted by ultrafiltration or dialysis, and then dissolved in 10 % formic acid (v/v). (Figure S1)

Simulation of molecular structure

The initial coordinates for the variants were constructed based on the crystal structure of the oxidation state of yeast iso-1-cytochrome c (pdb entry: 2YCC[S3]). The amino acid sequences were changed to those of the variants with VMD program.[S4] Water molecules were retained in the simulation. Force field parameters for the heme were described elsewhere[S5] and the peptides were simulated with CHARMM force field.[S6, S7] The structures of mutants were first minimized for 5000 steps with conjugate gradient method, and equilibrated for 10 ps with the time step of 1 fs, then were further minimized for 50,000 steps for analysis with VMD program. NAMD program[S8] was used for simulations (Figure S2). The energies did not change after 20,000 steps in the simulations of the variants (Figure S3).

UV–Visible spectroscopy

The UV-Visible spectra of the variants were recorded on a Hewlett-Packard 8453 diode array spectrometer equipped with a Neslab RTE-111 water circulator, controlled by laboratory software. Proteins were dissolved in 100 mM sodium phosphate buffer, pH 7.0. Protein concentrations were determined by using the pyridine hemochrome method.[S9] As shown in Figure S4, wild-type cyt c and the Y67H variant possess a weak

charge-transfer band centered at approximately 695 nm in the oxidized states, which is the characteristic of heme-Met80 coordination. The Y67H/M80V variant possesses a small peak around 627 nm in the oxidized state, which is the characteristic of high-spin ferric heme protein.

EPR spectroscopy

Samples were analyzed by X-band EPR on a Bruker EMX EPR spectrometer fitted with a Hewlett Packard 5352B microwave frequency counter. A standard Bruker cavity (ER4102ST) was used in conjunction with an Oxford Instruments ER910A cryostat for low temperature analysis. The temperature for the samples was 10 K; the buffer was 20 mM in sodium phosphate (pH 7.0); the microwave power was 2.02 mW. (Figure S5)

pH titration

Protein samples were prepared in the mixture of sodium phosphate and sodium borate buffers ([protein]≈5 μM, ionic strength=0.1 M) for the alkaline titration, and in the mixture of sodium phosphate, sodium acetate and sodium chloride buffers (20 mM each) for the acid titration, and titrated with increasing amounts of 12 M NaOH or 10 M HCl at 25 °C. The progress of titration was monitored by Hewlett-Packard 8453 spectrometer. The pH values were measured directly in the cuvettes using a Schott microelectrode (type 16PH) connected to an Orion pH meter (type 310P-02).

The basification of the Y67H variant could be monitored at 695 nm, which is the characteristic of the heme-Met80 coordination. The Y67H/M80V and Y67H/M80D variants do not possess this coordination and thus the titrations were monitored at 400 nm, which was proved to reflect the same process with 695 nm.[14] The curve plotted from the changes in absorbance with increasing pH values were analyzed using the equation below:

$$y = \frac{A_L * 10^{(pK-x)*n} + A_H}{1 + 10^{(pK-x)*n}}$$

, where A_L is the absorbance of the native state and A_H is the absorbance at the alkaline conformer. For the Y67H variant, the analysis using the absorbance at 695 nm or at 400
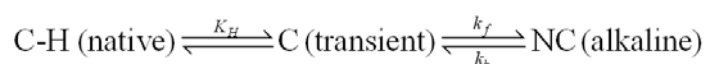
nm gave the identical pK_a value, 9.2, which further justified the monitoring at 400 nm (Figure S7). The pK_a values for the Y67H/M80V and Y67H/M80D variants are 8.6 and 10.3, respectively. The n value is 1.03 for wild-type cyt c, 0.95 for the Y67H variant, 0.82 for the Y67H/M80V variant and 0.89 for the Y67H/M80D variant.

Some interesting findings were obtained in the acid titration experiments (Figure S8). For the Y67H variant, the spectrum did not change upon decreasing the pH from 7.0 to 5.2. From 5.2 to 4.0, the absorbance at 695 nm underwent a sharp decrease while the absorbance at 620 nm increased only a little. With further decreasing the pH, the absorbance at 620 nm underwent a sharp increase, indicating the transition to the His18-heme-water coordination, which is comparable to the wild-type cyt c. This indicates that perhaps a low-spin intermediate was formed during the transition from the native Met80-coordinated state to the high-spin water coordinated state (in the pH range 5.2 to 4.0).

pH-jump kinetics

For the kinetics studies, protein samples (20 μM protein, 100 mM NaCl, pH 7 and unbuffered) were rapidly mixed with equal volume of buffer in a SF-61 DX2 stopped-flow apparatus (Hi-Tech, UK) thermostated at 25.0±0.1 °C. The following buffers were used: CHES (Sigma) (pHs 9.00, 9.10, 9.21, 9.29, 9.41, 9.51, 9.65, 9.78, 9.90 and 10.01) and CAPS (Sigma) (pHs 10.17, 10.37, 10.60 and 10.79). These buffers were prepared with sufficient NaCl to achieve the final ionic strength of 0.1 M.

The alkaline transition of cyt c is an intricate process which is now widely recognized to be consistent with a two-step mechanism. A minimal model can be used to describe this mechanism

$$\text{C-H (native)} \underset{}{\overset{K_H}{\rightleftharpoons}} \text{C (transient)} \underset{k_b}{\overset{k_f}{\rightleftharpoons}} \text{NC (alkaline)}$$

in which K_H stands for the dissociation constant of the first step, while k_f and k_b are the forward and reverse rate constants in the second step, respectively.

The rate constants of change in absorbance at 400 nm (k_{obs}) were obtained by fitting the stopped-flow curves to a first-order exponential function. The data can be fitted by the function below, as described by Davis $et\ al.$ (J. Biol. Chem. 1974, 2624-2632)

$$k_{obs} - k_b = \frac{k_f * K_H}{K_H + 10^{-pH}}$$

For wild-type cyt *c*, the experimentally measured rate constant at pH ~7 was used as an approximation for k_b. For the variants do not possess Met80-heme coordination, the pH-jump was monitored at 400 nm. However, although the changes at 400 nm reflect the same process with 695 nm, the absorbance changes are relatively small, making it impossible to obtain the first-order rate constant at pH<8. Hence the rate constants at pH 8.6 were used as k_b in our analysis (Y67H=0.2, Y67H/M80V=0.5, Y67H/M80D=1.2). These values are much larger than the k_b of the wild-type cyt c (~0.05), which is measured at pH 7 and monitored at 695 nm. It is a pity that this difference made the rate constants cannot exactly reflect the alkaline conformational transitions of the variants. However, as the variance in k_b cannot introduce large alteration in the K_H, we still list these values here. In our analysis, K_H for Y67H, Y67H/M80V and Y67H/M80D are 2.34×10^{-11}, 2.10×10^{-10} and 1.70×10^{-10}, respectively (Figure S9).

Stead-state kinetic studies

The steady-state kinetics of oxidation of guaiacol were studied with a SF-61 DX2 stopped-flow apparatus (Hi-Tech, UK) thermostated at 25.0 ± 0.1 ˚C. The H_2O_2 solution was prepared with 30% stock solution and its concentration was determined with an absorption coefficient of 39.4 $M^{-1}cm^{-1}$ at 240 nm.[S10] A solution of the variants (2.0 μM) and guaiacol (200 μM) in 100 mM buffer (pH 7.0, 8.0, 9.0 and 10.0, respectively) and a solution of 400 mM H_2O_2 in the same buffer were preincubated at 25.0 ± 0.1˚C for 5 min. Then, both solutions were mixed together in the mixing cell of the stopped-flow instrument to start the oxidation reaction. The steady-state reaction rates were obtained by monitoring the absorbance increase at 470 nm using a molar absorption coefficient of 26.6 $mM^{-1}cm^{-1}$.[S11, S12]

The product formation curve of guaiacol oxidation catalyzed by the variants is similar to that catalyzed by *Paracoccus versutus* cytochrome *c*-550[S13, S14] as shown in Figure S10, which exhibits an lag phase (I) before a linear phase (II), then followed by a decrease in activity (III) and finally a decrease in absorption. The rate of the steady-state reaction was determined by taking the maximum of the first derivative of the product formation curve (i.e. the linear phase).

The peroxidase activity vs. pH (pH 2-10) for the wild-type cyt *c* was also measured at 25.0 ± 0.1 ˚C (Fig. S11). The following buffers were used: 100 mM sodium phosphate buffer (pH 2.0, 3.0 and 6.0-8.0), 100 mM sodium acetate buffer (pH 4.0-6.0), 100 mM

sodium borate buffer (pH 8.5-10.0); 1 µM protein, 100 µM guaiacol, 200 mM H_2O_2. Although the activity is pH dependent, as the highest activity at pH 3 (k=0.030 AU_{470}/s) and lowest at pH 5 (k=0.011 AU_{470}/s) in our analysis, it is reported that the peroxidase activity could increase more than 50 times when undergo pro-apoptotic conformational transition.[4b,11] Thus, if some conformer or intermediate in the pro-apoptotic route emerges during the alkaline transition, the peroxidase activity would surely undergo a sharp increase. This result further evidenced the statement in the manuscript.

[S1]   W.B. Pollock, F.I. Rosell, M.B. Twitchett, M.E. Dumont and A.G. Mauk,   Biochemistry 37 (1998) 6124-31.

[S2]   F.I. Rosell and A.G. Mauk,   Biochemistry 41 (2002) 7811-8.

[S3]   A.M. Berghuis and G.D. Brayer,   J Mol Biol 223 (1992) 959-76.

[S4]   W. Humphrey, A. Dalke and K. Schulten,   J Mol Graph 14 (1996) 33-8, 27-8.

[S5]   F. Autenrieth, E. Tajkhorshid, J. Baudry and Z. Luthey-Schulten,   J Comput Chem 25 (2004) 1613-22.

[S6]   A.D.J. MacKerell, D. Bashford, R.L. Bellott, R.L. Dunbrack, Jr. , J.D. Evanseck, M.J. Field, S. Fischer, J. Gao, H. Guo, S. Ha, D. Joseph-McCarthy, L. Kuchnir, K. Kuczera, F.T.K. Lau, C. Mattos, S. Michnick, T. Ngo, D.T. Nguyen, B. Prodhom, W.E. Reiher, III, B. Roux, M. Schlenkrich, J.C. Smith, R. Stote, J. Straub, M. Watanabe, J. Wiorkiewicz-Kuczera, D. Yin and M. Karplus,   J Phys Chem B 102 (1998) 3586-616.

[S7]   A.D. Mackerell, Jr., M. Feig and C.L. Brooks, 3rd,   J Comput Chem 25 (2004) 1400-15.

[S8]   L. Kale, R. Skeel, M. Bhandarkar, R. Brunner, A. Gursoy, N. Krawetz, J. Phillips, A. Shinozaki, K. Varadarajan and K. Schulten,   J Comput Phys 151 (1999) 283-312.

[S9]   E.A. Berry and B.L. Trumpower,   Anal Biochem 161 (1987) 1-15.

[S10]   D.P. Nelson and L.A. Kiesow,   Anal Biochem 49 (1972) 474-8.

[S11]   D.A. Baldwin, H.M. Marques and J.M. Pratt,   J Inorg Biochem 30 (1987) 203-17.

[S12]   G.D. DePillis, B.P. Sishta, A.G. Mauk and P.R. Ortiz de Montellano,   J Biol Chem 266 (1991) 19334-41.

[S13]   R.E. Diederix, M. Ubbink and G.W. Canters,   Eur J Biochem 268 (2001) 4207-16.

[S14]   R.E. Diederix, M. Fittipaldi, J.A. Worrall, M. Huber, M. Ubbink and G.W. Canters,   Inorg Chem 42 (2003) 7249-57.
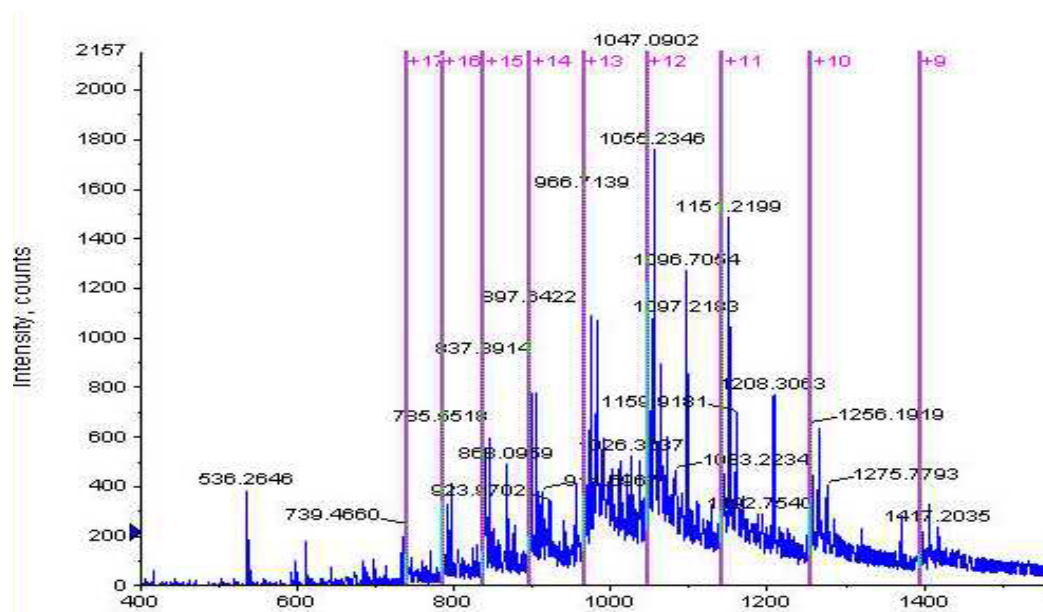
Figure S1. ESI-MS of the Y67H/M80V variant, the measured molecular weight is 12552±6 dalton. (calculated molecular weight: 12550). For the Y67H variant, the measured molecular weight is 12574±6 dalton (calculated molecular weight: 12581). For the Y67H/M80D variant, the measured molecular weight is 12565±6 dalton (calculated molecular weight: 12566).
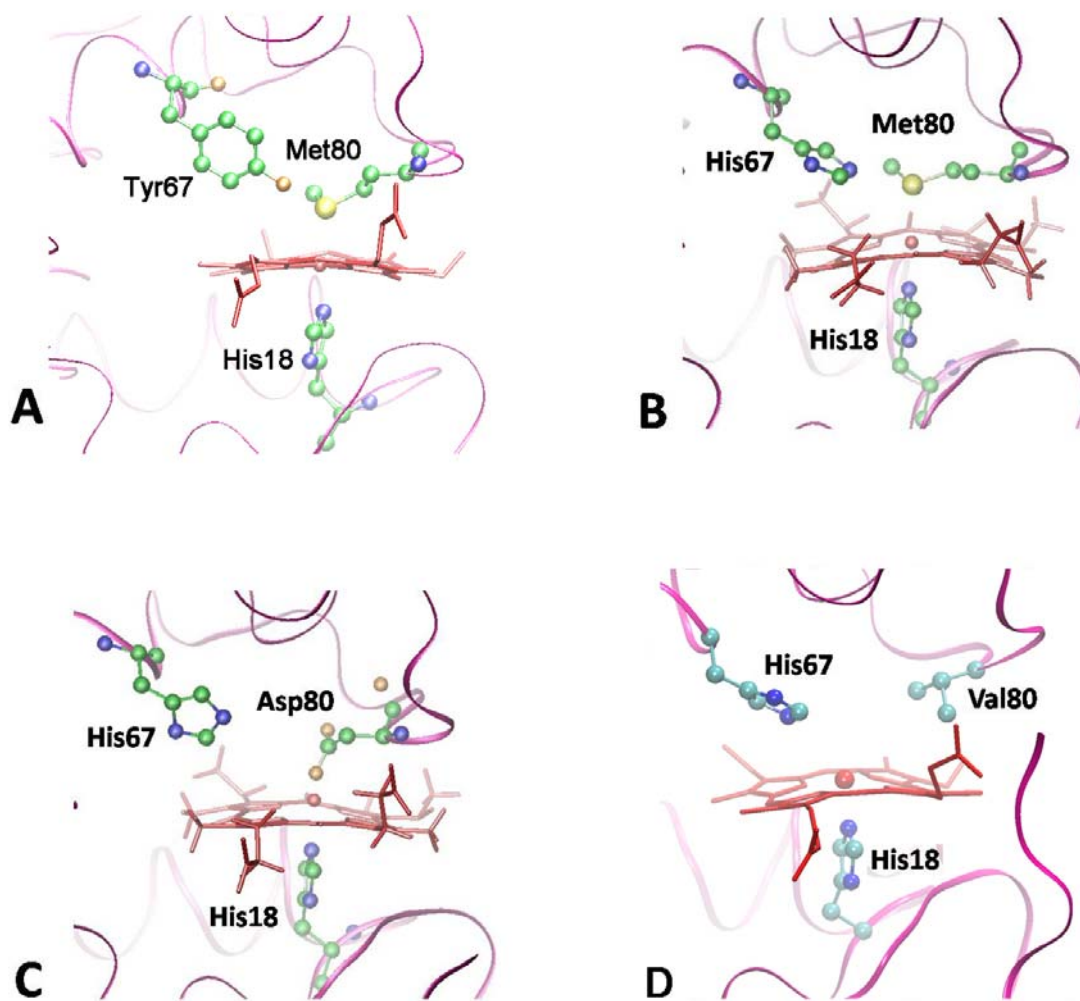
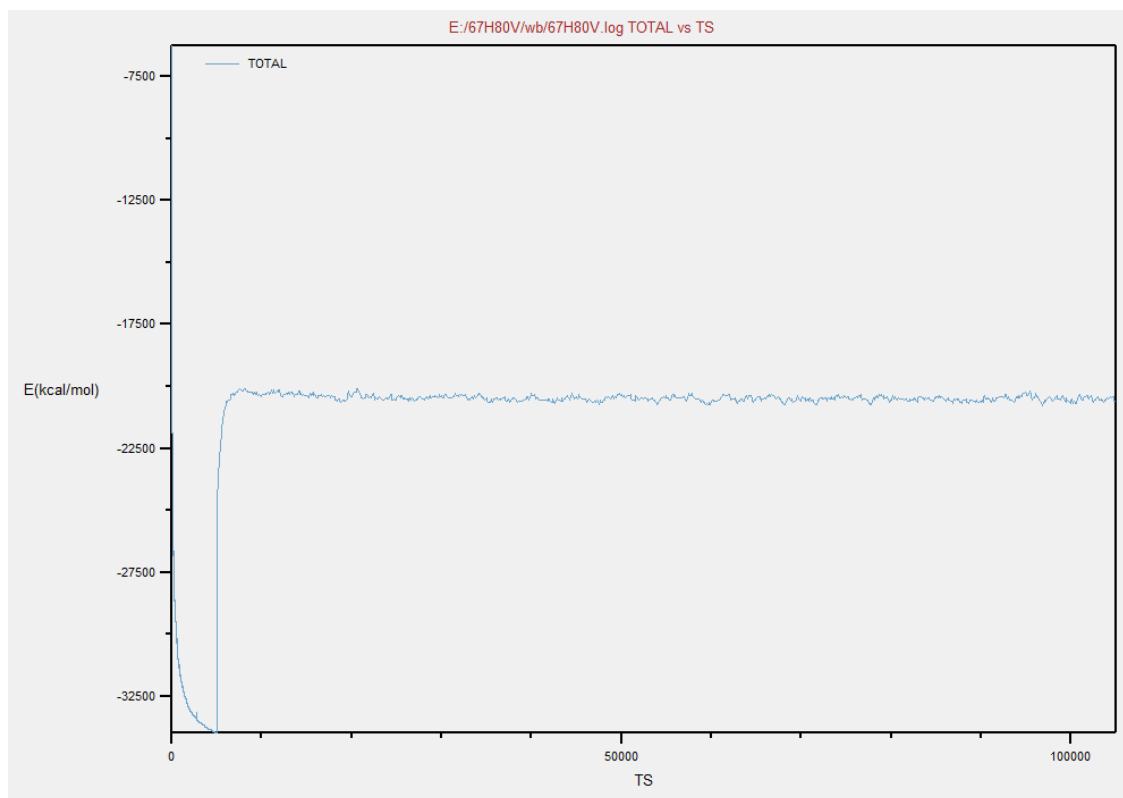**Figure S2.** Structure of yeast iso-1 cyt *c* (PDB id: 2ycc) (A) and energy-minimized models of the Y67H (B), Y67H/M80D (C) and Y67H/M80V (D) variants.

Figure S3. Plot of the total energy (E) versus the time step (TS) in the MD simulation of the Y67H/M80V variant.
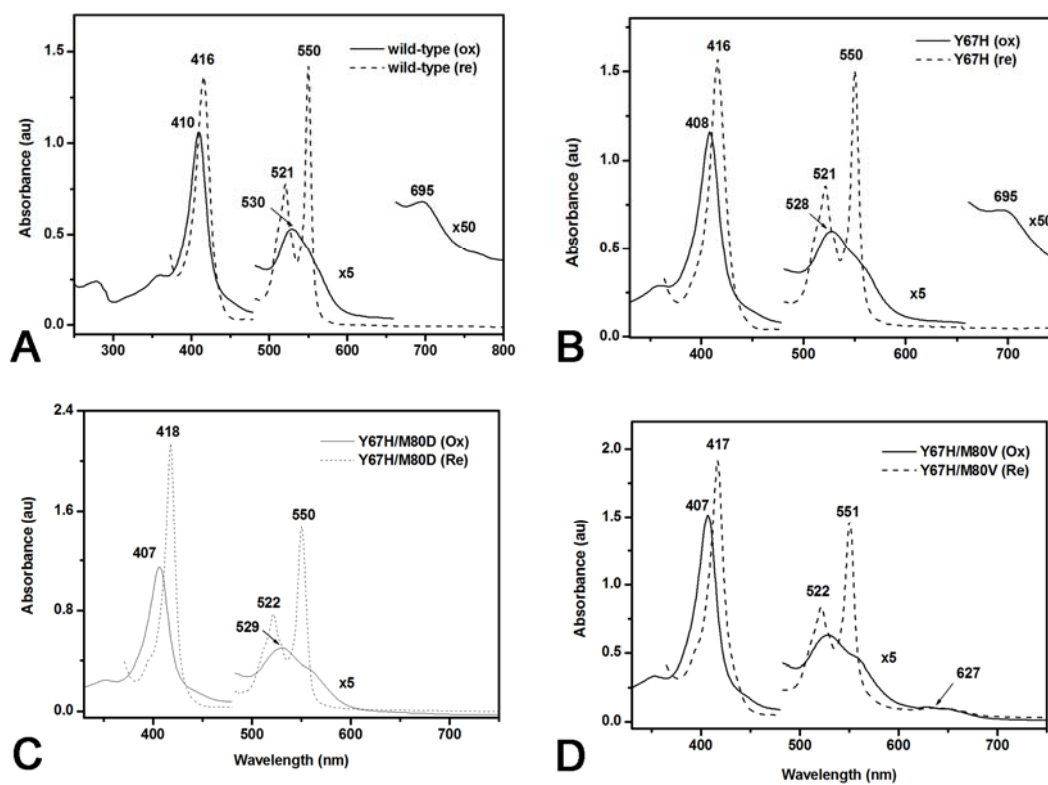
Figure S4. UV-Vis absorption spectra of (A) wild-type cyt *c*, (B) Y67H, (C) Y67H/M80D, (D) Y67H/M80V variants in the oxidized (— solid) and reduced (--- dashed) states. Protein concentration: 10 μM in 100 mM phosphate buffer (pH 7.0) at 25 °C.
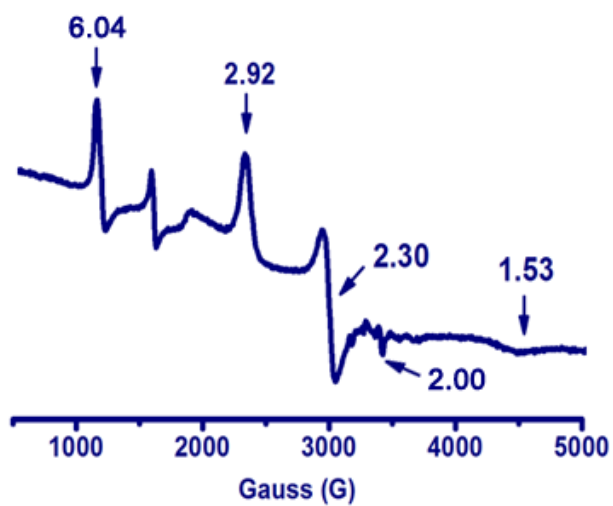
Figure S5. EPR spectrum of the Y67H/M80V variant at neutral pH (pH=7.0).
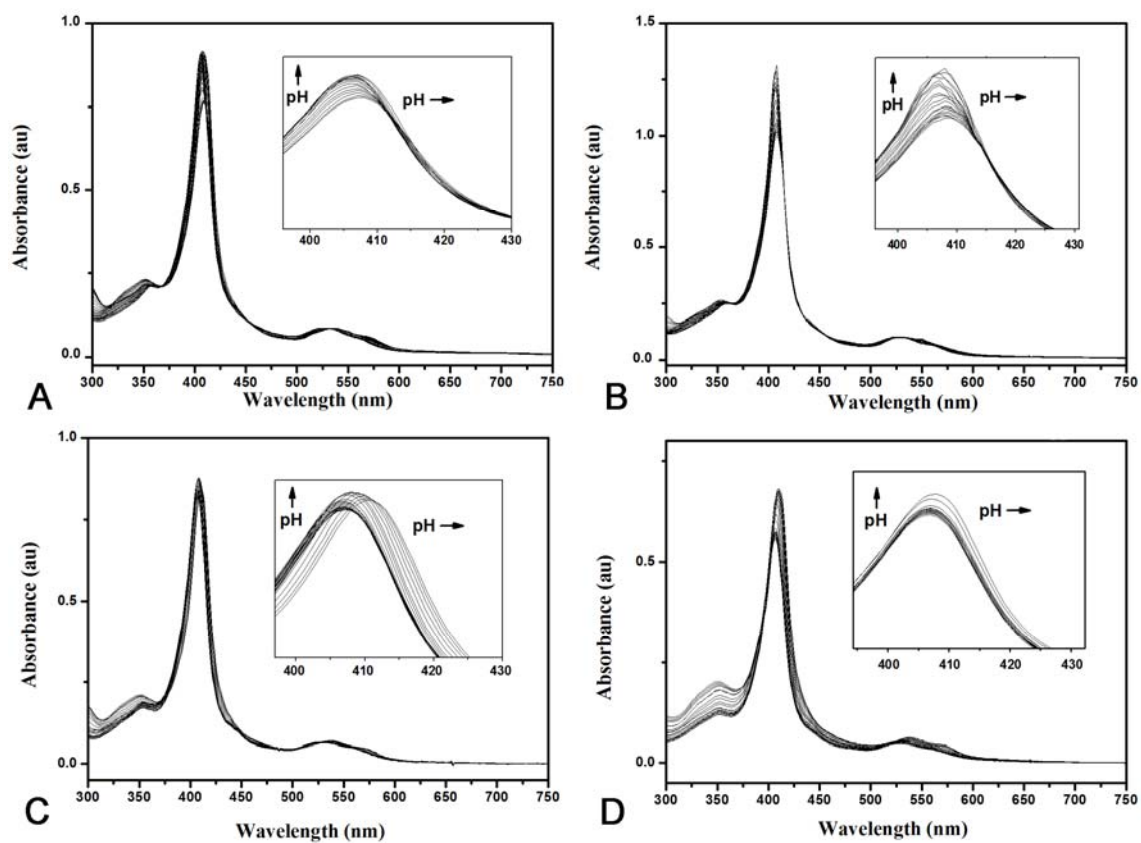
Figure S6. The alkaline titration of the ferric form of wild-type cyt *c* (A), the Y67H(B), Y67H/M80V(C) and Y67H/M80D (D) variants. The absorption spectra in the Soret region were enlarged and shown in the insets.
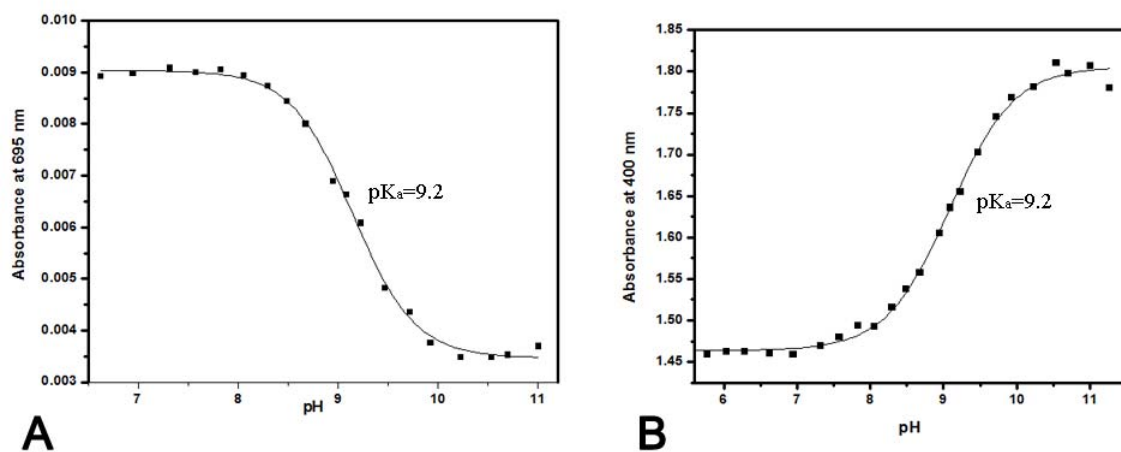
Figure S7. Absorbance changes at 695 nm (A) and 400 nm (B) as a function of pH values for the Y67H variant (25ºC, ionic strength=0.1 M, [Y67H]=20 μM).
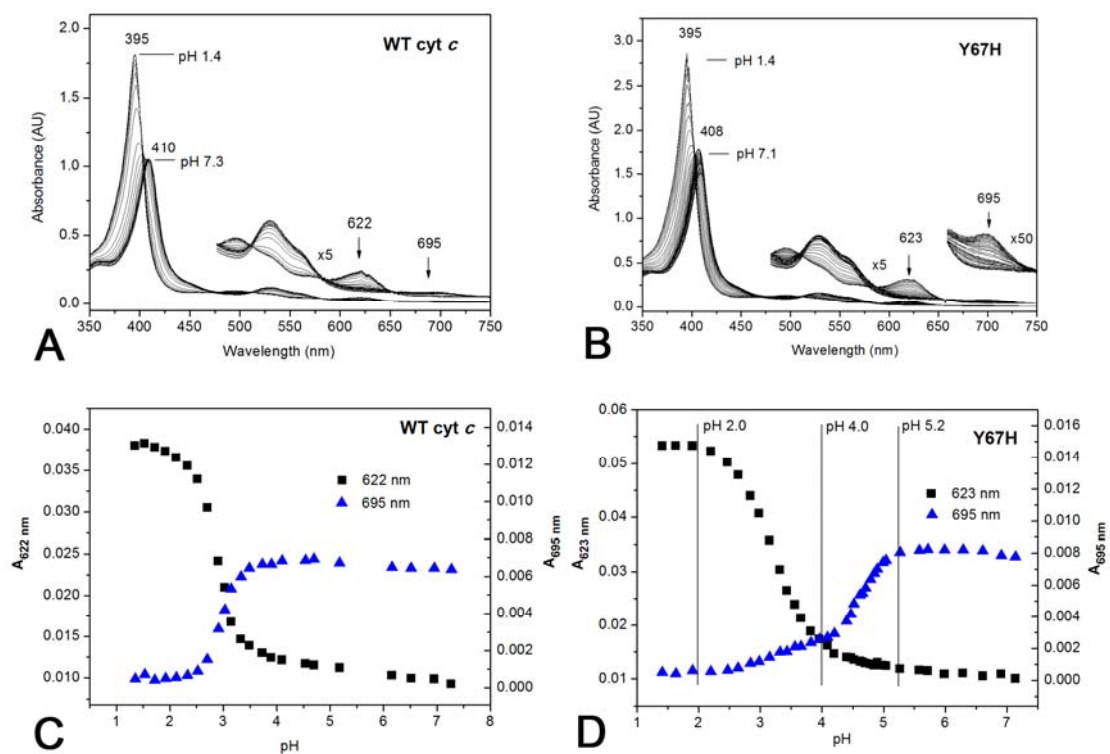
Figure S8. The acid titration of the ferric form of wild-type cyt *c* (A and C) and the Y67H variant (B and D). Conditions: Temperature 25°C, the buffer was 20 mM each in sodium phosphate, sodium acetate and sodium chloride.
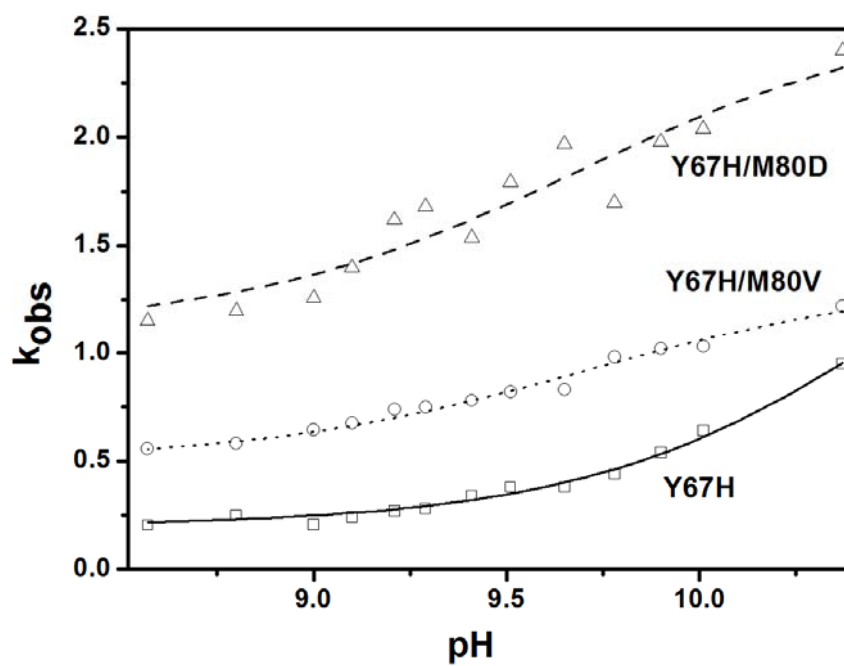
Figure S9. pH-jump kinetics of the Y67H (□), Y67H/M80V (○) and Y67H/M80D (△) variants. Each point represents the average of at least three determinations.
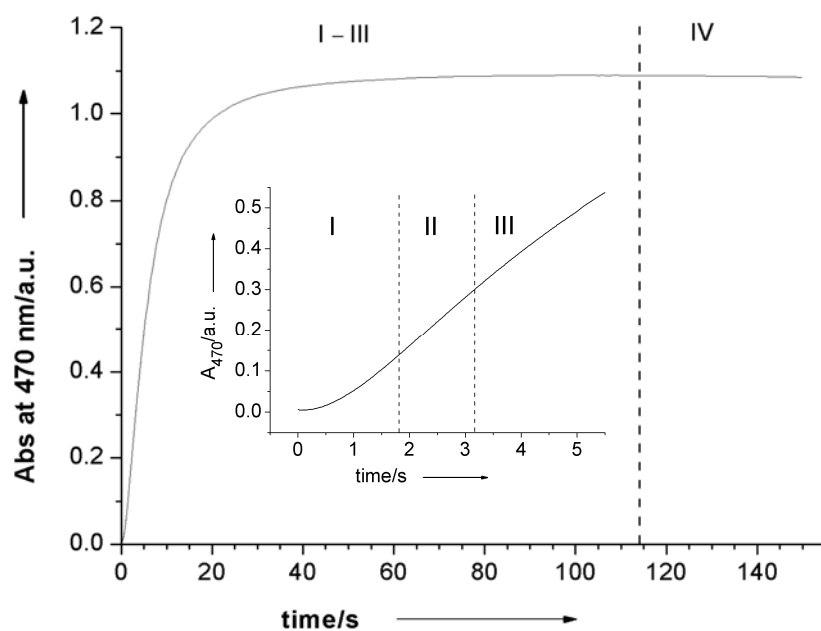
Figure S10. A formation curve of typical guaiacol oxidation product, tetraguaiacol, monitored at 470 nm. Conditions: 1 µM protein, 1 mM guaiacol, 75 mM H_2O_2 in 100 mM sodium phosphate buffer (pH 6.0) at 25.0 ± 0.1 °C. (Inset) The first 5-second curve of the product formation. The four phases labeled I–IV are explained in text.
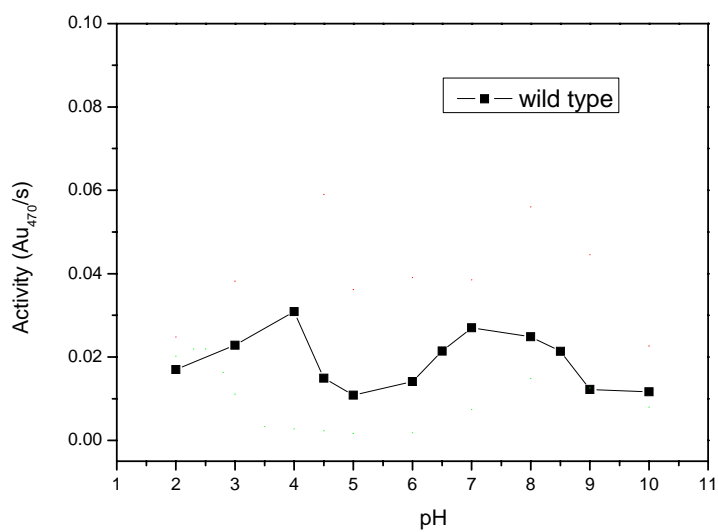
Figure S11. pH dependence of the peroxidase activities of the wild-type cyt *c*. The following buffers were used: 100 mM sodium phosphate buffer (pH 2.0, 3.0 and 6.0-8.0), 100 mM sodium acetate buffer (pH 4.0-6.0), 100 mM sodium borate buffer (pH 8.5-10.0); 1 μM protein, 100 μM guaiacol, 200 mM H_2O_2.